Cells and Materials

Volume 3 | Number 1 Article 10

1993

A Scanning Electron Microscope Study of the Ultrastructural Organization of Bone Mineral

F. B. Bagambisa
Freiburg University

U. Joos
Freiburg University

W. Schilli
Freiburg University

Follow this and additional works at: https://digitalcommons.usu.edu/cellsandmaterials

 Part of the Biomedical Engineering and Bioengineering Commons

Recommended Citation

Bagambisa, F. B.; Joos, U.; and Schilli, W. (1993) "A Scanning Electron Microscope Study of the Ultrastructural Organization of Bone Mineral," *Cells and Materials*: Vol. 3 : No. 1 , Article 10.
Available at: https://digitalcommons.usu.edu/cellsandmaterials/vol3/iss1/10

This Article is brought to you for free and open access by the Western Dairy Center at DigitalCommons@USU. It has been accepted for inclusion in Cells and Materials by an authorized administrator of DigitalCommons@USU. For more information, please contact digitalcommons@usu.edu.

Cells and Materials, Vol. 3, No. 1, 1993 (Pages 93-102)
Scanning Microscopy International, Chicago (AMF O'Hare), IL 60666 USA

1051-6794/93$5.00+.00

A SCANNING ELECTRON MICROSCOPE STUDY OF THE ULTRASTRUCTURAL ORGANIZATION OF BONE MINERAL

F.B. Bagambisa*, U. Joos, W. Schilli

Department of Oral and Maxillofacial Surgery, Freiburg University,
Hugstetterstr. 55, W-7800 Freiburg, Federal Republic of Germany.

(Received for publication December 10, 1992, and in revised form March 29, 1993)

Abstract

Scanning electron microscopy (SEM) was used to study samples of lamellar bone at magnifications typical for the published transmission electron micrographs, to gain more insight into the three-dimensional ultrastructure of bone mineral. Untreated (whole bone) samples allowed an assessment of the degree of mineralization. Deproteinized samples revealed the ultrastructural form and organization of bone apatite to be a function of the extent to which collagen fibers were imbibed with mineral. Numerous parallel formations reminiscent of troughs, gutters, or furrows, pierced and traversed the mineralization front. These troughs showed varying diameters identifiable with collagen fibers, and were separated from one another by an elaborate system of thin platy septa and flakes. The troughs were interpreted as impressions of dissolved collagen fibers and bundles.

Confluencing calcospherites were characterized by rod-shaped and fusiform mineral aggregates with diameters complying with collagen fibers and bundles. Mature mineral showed no plates; it was characterized by bundles of vermiform particles.

It is suggested that in newly deposited bone mineral, mineral aggregates incompletely encrust collagen fibers and bundles, forming perifibrillar and interfibrillar plates and sheaths. During further mineralization these aggregates appears to coalesce to a continuous mineral phase.

Key Words: Bone apatite, crystal size, biomineralization, calcospherites, scanning electron microscopy, specimen preparation, deproteinization, hydrazine, sodium hypochlorite, collagen.

*Address for correspondence:
F. B. Bagambisa,
Department of Oral and Maxillofacial Surgery,
Freiburg University,
Hugstetterstr. 55,
W-7800 Freiburg, Federal Republic of Germany.
Telephone No.: (0761) 2704701
FAX No.: (0761) 2704800

Introduction

The calcium phosphate minerals in dental enamel, dentin and bone are taken to be composed of hydroxyapatite. It is agreed that this *in vivo* apatite occurs solely in form of crystallites generally less than a few tens of nanometers. But there is no general consensus on the habit or dimensions of the crystallites. This is particularly true of bone mineral, whose crystallites are depicted as much smaller than in dentin and tooth enamel.

The prevalent views are three-fold: (**a**) bone mineral is not made up of individual crystallites, but rather a continuous ultraskeleton (Ascenzi and Chiazzoto, 1955; Turner and Jenkins, 1981); (**b**) bone mineral is made up of discrete crystallites with a needle- or rod-shaped habit; (c) bone mineral is made up of crystallites with a platy (tabular) form. There is a fourth discrepancy: (**d**) the crystallite sizes as determined by transmission electron microscopy (TEM) tend to be larger than those determined by X-ray diffraction.

On the basis of TEM, Robinson and Watson (1952) and Robinson (1955) concluded that bone apatite crystallites have a tabular form, mature crystallites having average dimensions of 150.0 x 50.0 x 10.0 nm. Fernández-Morán and Engström (1957), on the other hand, interpreted their TEM results to indicate a needle- or rod-shaped crystallite habit. Apart from these rods of dimensions 3.0-6.0 x 10.0 nm, they also described crystallite flakes measuring 2.0-5.0 by 30.0-50.0 nm, which they accounted for as lateral aggregations of the rods. Bocciarelli (1970) found crystallites of 2.0-4.0 nm diameter and a length of a few tens of nm. This author also observed platy crystallites (60.0-70.0 nm in diameter), which she interpreted as evidence for the presence of octacalcium phosphate in bone mineral. Schwarz and Pahlke (1953) reported oval or spindle-form particles with dimensions ranging from 15.0 to 130.0 nm.

X-ray diffraction investigations on bone material have corroborated both the needle-like and the platy habit of the apatite crystallites in bone, with the longest dimension of the crystallites (corresponding to the c axis) lying parallel to the axis of the collagen fibers (Stühler, 1938; Münzberg, 1970).

Although TEM and X-ray diffraction have made

a tremendous contribution to our understanding of mineralized tissues, we have to concede that both methods have their inherent limitations, certainly in the quest to understand the three-dimensional ultrastructure of the brittle, dense and heterogeneous inorganic fraction of bone. Even if artifacts like mineral shattering introduced during ultramicrotomy could be corrected for, the ultrathin sections mandatory for TEM investigation as well as the transmission mode itself allow essentially only a two-dimensional reproduction of structural information.

The conclusiveness of data obtained from X-ray diffraction studies is compromised when the samples employed have to be calcinated and/or powdered before they can be investigated. Powdering has been held responsible for fragmentation of apatite crystals, at least in dental enamel (Daculsi *et al.*, 1984)

It appeared desirable to investigate whether a complementary application of SEM to the study of bone mineral ultrastructure can be advocated. The proposal seemed tenable because SEM has facilities suitable for the morphological investigation of a heterogeneous material like bone: it has a large depth of focus, is capable of rendering adequate resolution at magnifications routinely used in TEM, and it allows the ultrastructural study of bulky specimens without orientational difficulties.

This study has used the SEM criteria established by Boyde (1972) and Dempster *et al.* (1979) to identify the different surfaces in the remodelling process. However, a SEM with a field emission cathode has been used to achieve magnification ranges comparable with those published in TEM studies.

Materials and Methods

The bone samples used were obtained from human maxilla and from femoral diaphyses of adult alsatians.

Human bone

Thin bone chips (up to 4 mm in diameter) chiselled from the maxillary tuberosity region of a healthy adult male during surgical removal of impacted upper third molars were immediately suspended in pure, anhydrous hydrazine (Serva Feinbiochemica, Heidelberg, Germany) and kept at 60°C for 24 hours. After the deproteinization, the samples were air-dried in a fume cupboard, fixed onto aluminium stubs and examined in a Hitachi S-800 either uncoated or after sputter coating with 3.0-4.0 nm of gold.

Dog bone

After perfusion fixation with 2.5% glutaraldehyde in 0.1 M cacodylate buffered at 7.4 pH., the femora were disarticulated and 3-4 mm thick discs cut from the bone shaft using a hand saw. The samples were post-fixed overnight at 4°C in the same fixative, rinsed thoroughly in deionized water and prepared as whole bone or deproteinized (anorganic) specimens.

Whole bone

Following post-fixation and rinsing, the samples were equilibrated in an ascending series of ethanol and dried in a Balzers CPD 20 critical point dryer.

Anorganic samples

After post-fixation and rinsing of the samples, they were deproteinized (for 12-18 hours) using 5% sodium hypochlorite (NaOCl) in 0.1 M cacodylate buffered at a pH of 7.4. The specimens were then dehydrated and critical point dried as above.

Whole bone and anorganic specimens were then fractured, mounted onto aluminium stubs, coated with 7.0 nm of gold and viewed in a thermoionic cathode SEM (Cambridge Stereoscan) or coated with 3.0-4.0 nm and viewed in a field emission cathode SEM (Hitachi S-800). The low-voltage facility of the Hitachi S-800 was used to investigate uncoated specimens. The Hitachi S-800 was operating at working distances between 5 and 7 mm, emission current of 10 μA, an aperture of 30 μm and a vacuum of about 10^{-7} Torr. The probe current at accelerating voltages between 20 and 30 kV was about $2x10^{-9}$ A.

Results

Whole bone

At the mineralization front, the calcospherites were obscured by non-fibrillar organic material and bridged by what appeared to be collagen fibers (Fig. 1), comparable to those identified by Sela and Boyde (1977).

The resting surfaces presented a morphology seemingly indicative of the degree of mineralization (Fig. 2). In less mineralized sites, individual collagen fibers could be more easily distinguished, with the suggestion of periodic cross striations characteristic of bone collagen. In sites more densely infiltrated with mineral, individual fibers as well as the cross striations were less well marked. Fig. 2 also shows that the fibers and bundles have a granular surface and that they sometimes bulge and club along their lengths.

Deproteinized specimens

At low magnification, the samples showed a variegation of mineralization fronts, resting and resorbing surfaces (Fig. 3), with their typical SEM appearances at slightly higher magnifications (Figs. 4, 5). When the respective surface types were viewed at higher magnifications as routinely used in TEM, invariably, reproducible patterns emerged. In young anorganic bone, the surface of calcospherites depicted formations reminiscent of grooves, troughs or gutters suggesting impressions of the dissolved collagen fibers and bundles (Figs. 6-8). Bone mineral associated with loosely packed collagen fibers showed individual gutters; on the other hand, the mineral associated with collagen packed together in bundles had the appearance of one continuous mass, on whose surface plates and flakes could be discerned (Fig. 7). The edges of the troughs and flakes

Figure 1. Mineralization front in an untreated (whole bone) sample from dog diaphysis. Although the calcospherites are extensively obscured by organic material, they are still recognizable. Some of them are bridged by fibrillar structures (e.g., at arrows), most likely collagen fibers. Bar = 3.0 μm.

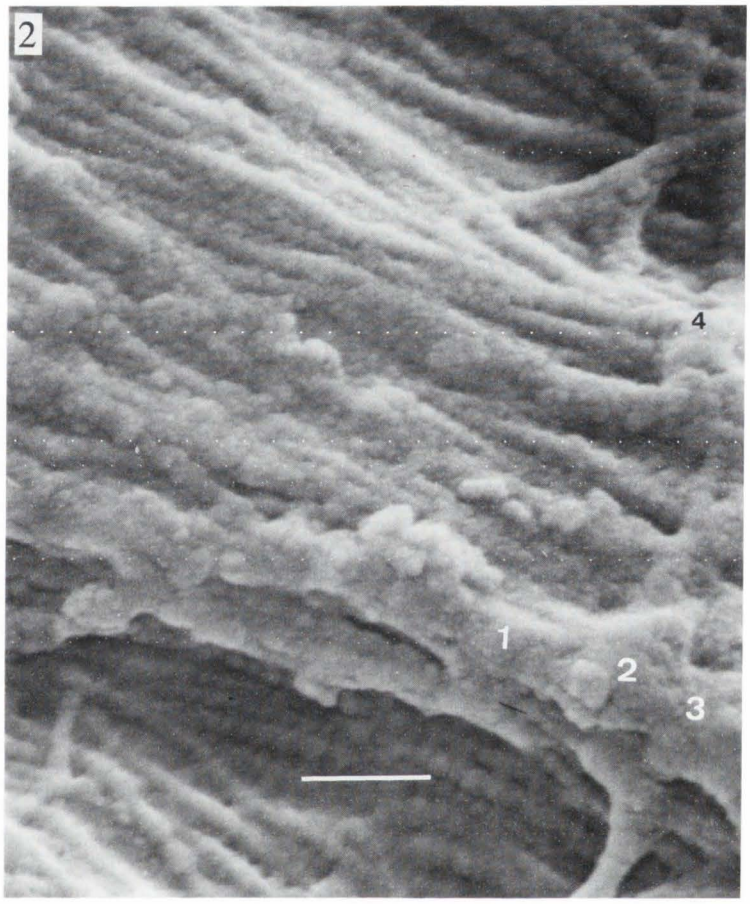

Figure 2. Resting bone surface in a sample of whole bone from dog femur diaphysis. Diagonally from upper left to lower right, the collagen fibers form a bundle in which mineral is densely invested, sometimes causing bulging and clubbing of the fibers (e.g., 1-4). Collagen periodicity is less discernible. Upper right and lower left are areas between neighboring bundles. Here the fibers are more loosely packed and the suggestion of collagen periodicity is more apparent. The surface is granular and some of the granules are assembled in clusters. Bar = 400 nm.

---

were sometimes serrated and/or curved-in (Figs. 6, 7), presumably tracing the curvature of the fibers, or bundles they ensheathed before deproteinization. Figs. 9 and 10 illustrate clearly that the calcospherites are not solid masses, but rather represent elaborate compartmentalized shells with grooves and canals running parallel to their long axes.

In confluencing calcospherites, occasionally, platy aggregates of irregular size and shape could be identified on the calcospherite surfaces (Fig. 11). But generally, the trough-shaped mineral aggregates associated with loosely packed collagen (Figs. 7, 8) seem to have assumed the size and configuration of collagen fibers, with lengths of up to 1 μm (Fig. 12). Some of these rod-shaped or fusiform structures still retain shallow grooves so that they would be kidney-shaped in cross-section. This in contrast to the situation in younger bone, where the cross-section would be crescent- or C-shaped.

The mineral in mature bone, as seen on resting and resorbing surfaces, showed no plates, and the notion of discrete crystallites became more elusive. Here the surfaces showed predominantly endless bundles of vermiform mineral formations (Fig. 13). If anything was suggestive of substructural morphology, then it was a periodic segmentation responsible for the vermiform appearance.

While studying the crystals, we met with no morphological or structural characteristics peculiar to dog or human bone.

Discussion

Viable bone tissue is perpetually undergoing a cyclic microrepair process called remodelling, whereby secondary osteons are formed. Osteons, in formation, represent mineralization fronts, structurally analogous to the front in primary ossification. Because of this cyclic reparative process, fracture surfaces or sections

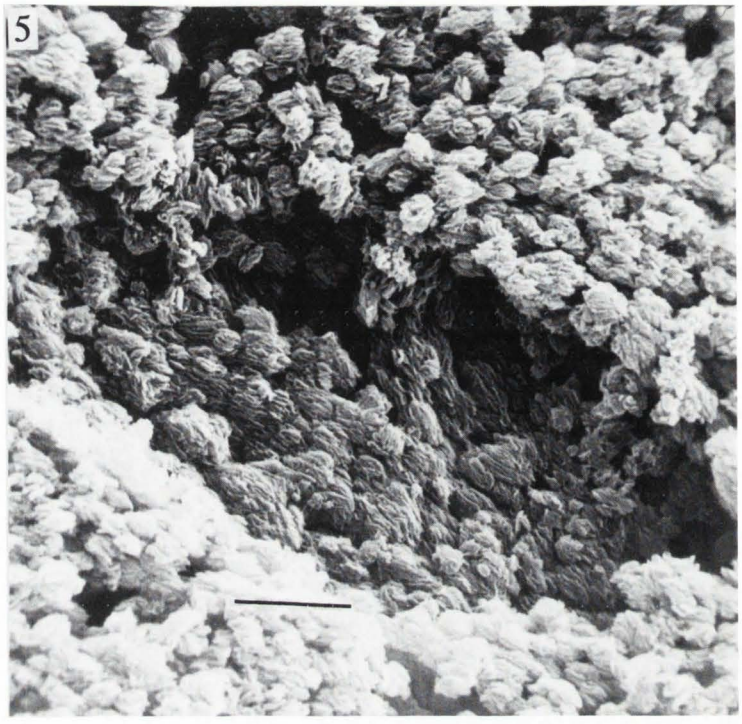

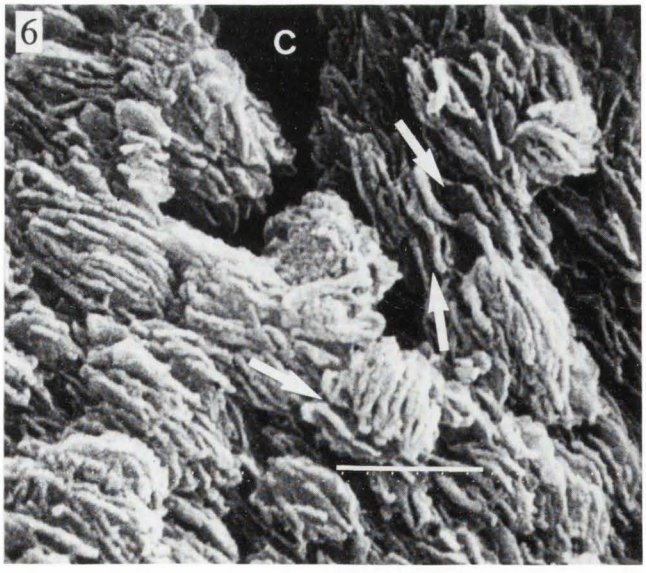

Figure 3. Heterogeneity of bone tissue. Hydrazine-deproteinized human jaw bone. A mineralization surface (left) is contiguous with a resorption surface. Howship's lacunae characterize the resorbing surface. Bar = 50 μm.

Figure 4. The typical appearance of a resorption surface at low magnification. The smooth texture (cf. Figure 5) and the scalloped edges of Howship's lacunae characterize this type of surface. NaOCl-treated surface from dog diaphysis. Bar = 20 μm.

Figure 5. Mineralization front in NaOCl-treated anorganic bone from dog diaphysis. Removal of the organic matrix exposes the calcospherites (cf. Figure 1). The micrograph is a depiction of an osteocyte lacuna under formation. The smoothly textured perilacunar mineral is not yet formed, implying that the mineral has been recently deposited. Bar = 3.0 μm.

Figure 6. Higher magnification of the middle of Figure 5. The surfaces of calcospherites show numerous troughs, (three troughs are marked with arrows) and plates (especially upper right). C, Canaliculus. Bar = 1.0 μm.

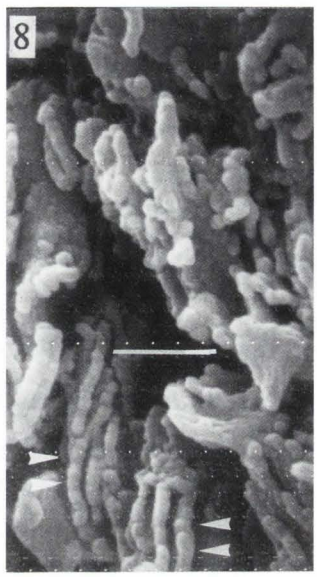

Figure 8. Mineralization front in dog bone made organic by NaOCl. The mineral surface presents with moniliform-edged trough formations (e.g., at arrowheads). Bar = 300 nm.

Figure 7. Mineralization front. Upper right, irregularly shaped plates (big arrows); upper left as well as below, predominantly troughs, (e.g., at smaller arrows). Bar = 250 nm.

---

of bone specimens present a mosaic of structural domains that have been well characterized in SEM by Boyde and Hobdell (1969), Boyde (1972) and Dempster *et al.* (1979). Fig. 3 depicts young bone characteristic of the mineralizing front extending like a peninsula into mature bone typical of the resorbing domains. Fig. 4 is a low-magnification micrograph of a mineralizing front illustrating calcospherites and Fig. 5 shows a resorption surface characterized by the scalloped edges of Howship's lacunae. The interpretation of the mineral ultramorphology in this study has been related to these domains.

The results presented here show that the ultrastructural topomorphology of bone mineral is highly elaborate and depends on the micromorphological zone in which the mineral is located: whether in young or mature bone domains. Given this complexity and the variegated nature of bone tissue and mineral, it becomes easy to appreciate the microscopic and ultrastructural orientational difficulties in TEM, and why the samples used in X-ray diffraction studies must invariably be heterogeneous.

At high magnifications, young bone was found to be composed of a continuous mass of mineral on whose surface irregularly shaped plates of colloidal dimensions could be identified (Figs. 6-10). Some of these plates seemed to be associated with collagen fibers closely packed together in bundles (Fig. 7, big arrows). In addition, trough-shaped mineral entities of varying length and diameter were identified, apparently associated with individual collagen fibers (Figs. 6, 8). With increasing mineral uptake, some plates and septa seem to become larger (Fig. 11) as most of the troughs get their hollows filled in with mineral, assuming rod-shaped or fusiform configurations with lengths up to 1 μm (Fig. 12).

In contrast, mature bone mineral is virtually void of mineral plates of any kind (Fig. 13); it is predominated by vermiform mineral masses suggesting "collagen skeletons" (Dempster *et al.*, 1979). There is no indication that these individual masses are hollow although a few of them would be kidney-shaped in cross-section as opposed to the crescent cross-section in young bone (Figs. 6-8).

The results seem to suggest that the mineralization of collagen fibers starts perifibrally, or at least within the peripheral (if integral) parts of the fibers, proceeds with penetration and imbibing of mineral into the substance of the fiber, forcing the fiber to bulge and increase in diameter (Fig. 2). If the structure of collagen is affected in this manner, its structure should be hardly discernible in fully mineralized bone sites.

Indeed this fact is borne with by three important observations: (**a**) a survey of the published transmission electron micrographs originating from **fully** mineralized zones shows that collagen fibers are almost never discerned; (**b**) in X-ray diffraction of whole bone, collagen gives a very weak background signal, or indication of collagen is missing altogether, so that the diffraction patterns of this tissue is predominated by apatite peaks (Stühler, 1938; Münzberg, 1970), and yet (**c**) after

decalcification of bone tissue the X-ray diagrams obtained are typical of collagen fibers (Stühler, 1938; Münzberg, 1970).

The colloidal plates (flakes) and perifibrillar mineral "cuffs" as demonstrated here in young bone as well as their apparent absence in mature bone have a bearing on observations made in TEM and with X-ray diffraction. An ultrathin section through the plane of Fig. 6 or 7 will meet the constellation of mineral particles in all sorts of planes. The plates will be sectioned parallel to their flat plane, askew or edge-on.

In a two-dimensional projection, most of these plates will appear like rods of varying lengths. This could substantiate the TEM findings (Johansen and Parks, 1960; Bocciarelli, 1970) that rod-like images were actually edge views of plate-like structures. Fig. 10 seems to make this interpretation almost inescapable. A section through Fig. 13, on the hand, would not show crystals. This corresponds to the published transmission electron micrographs of bone tissue. No crystals are found in domains other than the mineralizing front, immediately adjacent to osteoblasts. The present results seem to be at variance with the stipulation of Fernández-Morán and Engström (1957) that the plates they found were lateral aggregations of needle-shaped crystals.

Münzberg (1970) obtained diffraction patterns of single-crystals from young bone mineral. He concluded that these single apatite crystallites had to have dimensions of at least 50.0-100.0 nm in the c direction, otherwise their patterns would not have been resolved. Again it is noteworthy that this author never found single plates in mature bone mineral.

The technical data of the Hitachi S-800 guarantees a resolution of 2.0 nm for the instrument, so that the thickness of bone crystallites of the order of 2.0-5.0 nm as found in the literature should possibly have been resolved. Certainly, the acclaimed length of the needles or the length and breadth of the tabular crystallites would have been observed, since they are stated to be of the order of 20.0-100.0 nm. Although plates were found in the present study, no plate-plate grain boundaries (in a crystallographic sense) could be demonstrated (Fig. 10). Instead the plates were contiguous with solid masses of mineral. Further, the plates showed different radii of curvature, varying from an almost flat (Fig. 7, big arrow) to a c-shaped configuration (Fig. 6, 8). The differences in curvature most probably depend on whether the plates were encrusting single, or bundles of, fibers.

The plates were discerned only in young mineral. The shapes of these platy particles were so multifarious and the size distribution so uncertain that it would almost seem pretentious to make a statement any more precise than that the statistical average size of bone crystallites might be larger than has been hitherto assumed. Indeed, at least in mature bone domains, it seems more apt to revive the notion of a continuous mineral phase as suggested by Ascenzi and Chiazzotto (1955) and Barbour and Cook (1954).

Figure 9. Mineralization front in human jaw bone made anorganic with hydrazine. The micrograph shows that the calcospherites are not solid but enclose systems of channels running parallel to the calcospherites' long axes. Bar = 2.0 μm.

Figure 10. Higher magnification of the upper third of Figure 9. The canal systems going through the calcospherites and parallel to the latter's axes most likely represent impressions of the dissolved collagen fibers. Bar = 350 nm.

Figure 11. Mineralization front, confluencing calcospherites in dog femur bone. Plates of irregular shapes and sizes, some with one (A) and others with two (B) curved-in edges, can be discerned on a granular but continuous mass of mineral. Bar = 400 nm.

Figure 12. Mineralization front, confluencing calcospherites in NaOCl-deproteinized dog diaphysis. Although there are occasional structures still suggesting platy (P) and grooved (G) configurations, rod-shaped or fusiform mineral aggregates with diameters corresponding to collagen fibers and bundles are characteristic of this surface. The micrograph gives the impression that the collagen fibers previously partially impregnated by mineral has been dissolved, leaving behind the collagen "fibre skeletons" reported by Dempster *et al.* (1979). Note the granular appearance of the mineral aggregates. Bar = 300 nm.

Figure 13. Ultrastructural morphology of bone mineral associated with mature domains, originating from a Howship's lacuna. Dog diaphyseal bone made anorganic with NaOCl. There are no plates or rods apparent. The Figure gives the impression that collagen fibers previously impregnated by mineral along their entire visible length have been dissolved, leaving behind their mineral replica. Some substructures occur along the length of the "mineral skeletons" (apparently corresponding to collagen periodicity), lending them a vermiform appearance. Bar = 500 nm.

If bone is made up of such extremely small discrete crystallites of the order of 1.5-3.0 x 5.0-10.0 x 40.0-50.0 nm (Glimcher, 1984), one should expect a tremendous specific surface area of the mineral phase. The observation that the specific surface areas as measured in a variety of studies does not exceed 120 m^2/g might support the present finding that the discrete elementary particles of bone mineral, if they exist to any great extent, are (at least functionally) larger than has been hitherto anticipated, so that the "fused aggregates" reported by Weiner and Price (1986) are probably not aggregates of crystals but phase continua. If the particles identified here as granules (Figs. 2, 11, 12) and elsewhere in the literature are not artifacts, one wonders

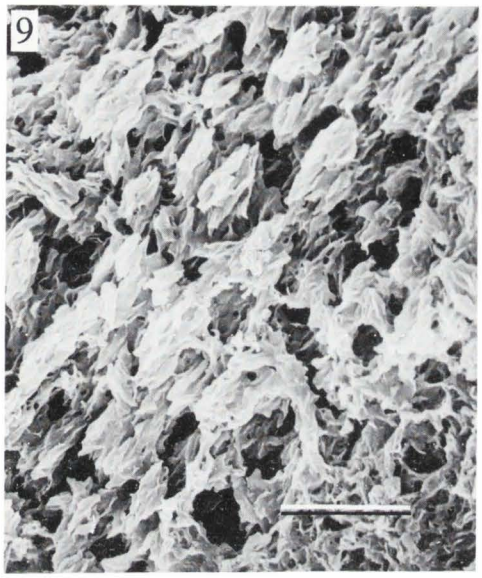
9

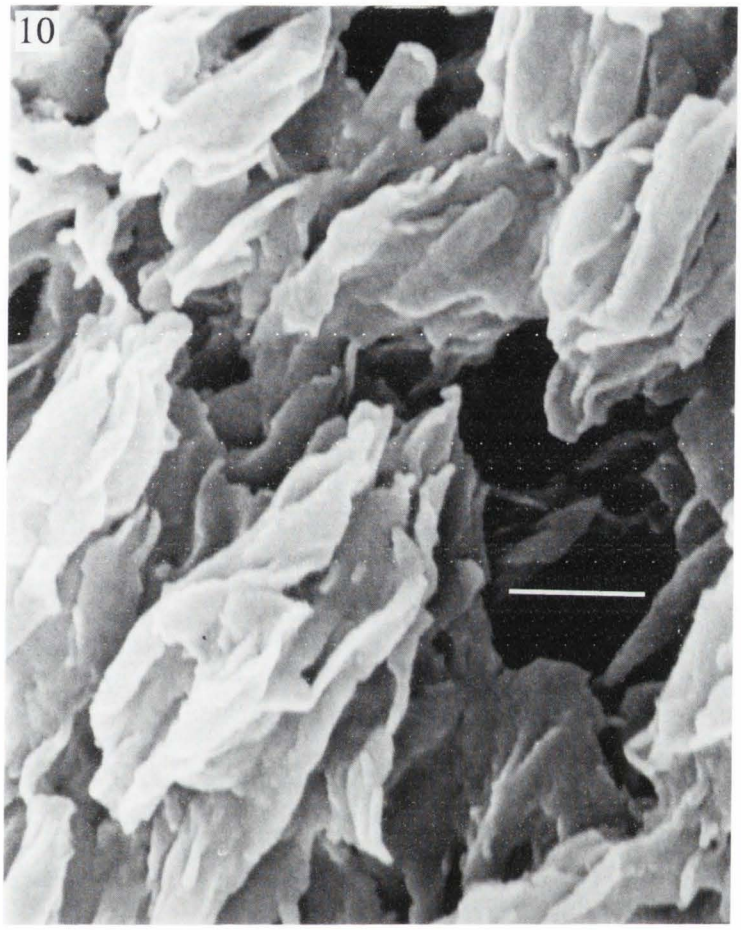
10

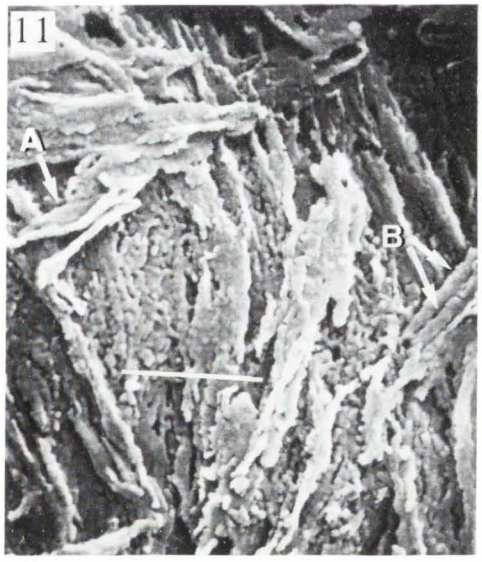
11
A
B

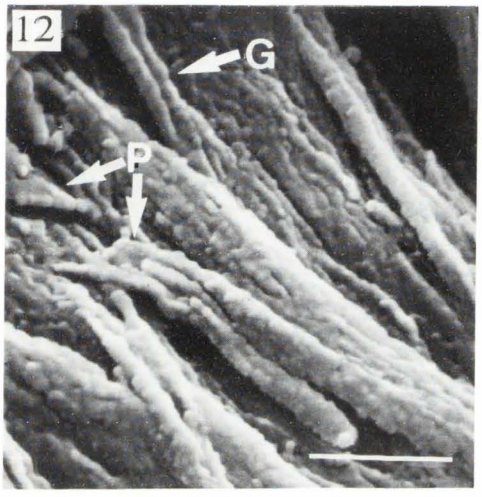
12
G
P


13

whether to consider them more as incremental particles rather than treat them rigorously as individual crystallites in the strict crystallographic sense that presupposes grain boundaries.

At the mineralization front, the earliest particles of bone mineral, which remain attached to the rest of the mineral mass after deproteinization, seem to be made up of plates completely or partially encircling the collagen fibers and bundles. In so doing, the long axis of these troughs is parallel to the long axis of the collagen fibers and bundles. These plates could be the "tabular crystallites" found in the literature on bone mineral morphology. The parallelity of the long axes of plates and collagen might be a corroboration of TEM and X-ray diffraction findings that bone crystallites lie with their c (long) axis parallel to the long axis of collagen fibers.

The present observations seem to be at variance with one of the prevalent opinions, that **mature bone mineral** is made up of infinitesimal discrete particles of the order of 1.5-3.5 x 5.0-10.0 x 50.0 nm. While the study cannot rule out the presence of such particles in the very initial mineral precipitated loosely in collagen, it seems to suggest that their presence in deproteinized mineral is unlikely. It tends to lead to the notion of a labyrinthous ultraskeleton of plates in newly deposited mineral, which, following further mineral apposition coalesces to form a more dense continuous phase.

Artifacts

The high source brightness associated with field emission cathodes allows microscopy at low accelerating voltages, without coating. Attempts to make micrographs from uncoated surfaces using the Hitachi S-800 at around 5 kV were successful only up to magnifications of 30,000. Micrographs taken at higher magnifications were fraught with specimen charging artifacts (in the form of image drift and horizontal dark stripes) of varying severity. The artifacts were most severe in young bone domains, most probably on account of the surface irregularities characteristic of these surfaces. We, therefore, tested thin coating and established that a coat of 5.0 nm gold was sufficient to operate at beam voltages of up to 30 kV. We did not observe heat-related artifacts. Although heat-related artifacts are more of a hazard with organic tissue than with the anorganic mineral, soft tissue components (Figs. 1, 2) seemed to display a normal morphology.

It should be noted that during deproteinization the initial mineral deposits physically associated only with collagen get lost with removal of the collagen scaffolding (Boyde and Sela, 1978). The terms "young bone" and "mineralization front" as used in this study refer, therefore, not to the very earliest mineral clusters deposited in osteoid but to the earliest clusters that remain attached to the rest of the mineral mass after deproteinization. It is in these clusters that no grain-grain boundaries could be demonstrated. Hence the suggestion that if the very initial particles (that get lost with dissolution of collagen) are isolated entities, this individuality seems to be lacking in the plates that remain attached to the rest of the mineral mass.

Two reagent quality agents were used for deproteinization in this study: an aqueous solution (NaOCl) and pure, anhydrous hydrazine. The observation has been made in TEM studies that exposure of mineralized bone tissue to aqueous media leads to translocation as well as loss of mineral (Boothroyd, 1964; Thorogood and Gray, 1975). However, this is a special problem of TEM introduced during thin sectioning and floating. Moreover, these artifacts seem to occur in the said zone that is lacking in anorganic SEM specimens, the mineral having been lost with the withdrawal of the mechanical support of collagen fibers.

Of more concern is the effect of the deproteinizing agents on the integrity of mineral morphology. It is reasonable to suspect that deproteinizing agents existing as water solutions attack the mineral phase, if, perhaps, to a limited extent. Since the calcium phosphates are sparingly soluble in water, the process of attack will not be just a one-way dissolution but more a (reversible) two-way dissolution/reprecipitation event. Weiner and Price (1986) concluded that exposure of bone mineral to NaOCl for up to 144 hours does not appreciably alter mineral morphology.

However, we have made the observation (unpublished results) that during deproteinization with NaOCl the surfaces of dental and bone mineral directly exposed to the solution develop a dissolution/reprecipitation layer. These surfaces are covered with spheritic mineral entities, about 20-50 nm in diameter. At the mineralizing front in bone, these spherites are organized in a hierarchy of primary, secondary and tertiary structures, rather reminiscent of a cauliflower head. Similar structures can be observed in bone specimens made inorganic by heating at 100°C or 700°C and then immersing in aqueous solutions of collagenase for a week (Green *et al.*, 1985, 1988). On fracture surfaces, these presumably artifactual spherites are generally absent (Figs. 6, 7, 11, 12), although they may be suggested in Fig. 8, where the edges of the troughs are moniliform. In hydrazine-treated specimens, there was no discernible suggestion of spherites (Figs. 9, 10).

The specimens were sputter coated with a nominal thickness of 7.0 nm for the Stereoscan and 3.0-4.0 nm for the Hitachi S-800. Because of the extremely non-planar nature of the surfaces investigated (see Figs. 5-13), no attempt has been made to correct for the coating thickness; moreover, no rigorous quantitative treatment has been instituted in the study to warrant consideration of the coating thickness. It is also for this reason that no stereo pair micrographs were prepared. It should be pointed out, however, that no coating structure was resolved on any of the specimens, and there seems to be no apparent cause to suppose that the coating obliterated any intercrystalline "grain boundaries" (Figs 6-8, 10 and 11).

We made the observation that hydrazine does not remove the entire protein moiety from bone tissue. We

are unable to speculate on the reasons for this. We changed the reagent copiously enough to ensure that it would not be ineffective because of being used up. Moreover, while in some domains, the calcospherites were partly obscured by residual protein, deproteinization was complete in the majority of others (Figs. 9 and 10). The incomplete removal of protein is in agreement with the findings of Walters *et al.* (1990) who obtained infrared spectroscopic bands attributable to residual protein in hydrazinolysed bone.

Conclusions

The present study suggests that the three-dimensional morphology, both at microscopic and at the ultrastructural levels of organization, is a function of the "age" of the domain under study, depending on whether one is dealing with a young or a mature site. In deproteinized bone, new mineral seems to be deposited between collagen fibers and bundles, partially or completely ensheathing them. During further mineral deposition, the mineral extends into fibers, and the individual mineral aggregates coalesce to a dense and continuous mineral mass. There is no apparent suggestion of individual crystal entities in mature bone domains.

SEM is one instrument with which the study of the different domains of the intrinsically heterogeneous bone (mineral) can be undertaken with certainty. Moreover, the SEM, especially if built with the biologist in mind, has the high resolution potential to allow the collection of morphological data rigorous enough to supplement and enhance our understanding of bone mineral at the ultrastructural level of organization.

References

Ascenzi A, Chiazzotto A (1955) Electron microscopy of the bone ground substance using the pseudoreplica technique. Experimentia **11**, 140-142.

Barbour EP, Cook SF (1954) The effects of low phosphorus diet and hypophysectomy on structure of compact bone as seen with the electron microscope. Anat. Rec. **118**, 215-230.

Bocciarelli SD (1970) Morphology of crystallites in bone. Calcif. Tissue Res. **5**, 261-269.

Boothroyd B (1964) The problem of demineralization in thin sections of fully calcified bone. J Cell Biol. **20**, 165-173.

Boyde A (1972) Scanning electron microscopic studies of bone. In: The Biochemistry and Physiology of Bone, Vol 1. Bourne GH (ed.), Academic Press, New York, 259-310.

Boyde A, Hobdell MH (1969) Scanning electron microscopy of lamellar bone. Z. Zellforsch. **93**, 213-231.

Boyde A, Sela J (1978) Scanning electron microscopic study of separated calcospherites from the matrices of different mineralizing systems. Calcif. Tissue Res. **26**, 47-49.

Daculsi G, Menanteau L, Kerebel LM, Mitre D (1984) Length and shape of enamel crystals. Calcif. Tissue Int. **36**, 550-555.

Dempster DW, Elder HY, Smith DA (1979) Scanning electron microscopy of rachitic rat bone. Scanning Electron Microsc. **1979**;II: 513-520.

Fernández-Morán H, Engström A (1957) Electron microscopy and X-ray diffraction of bone. Biochim. Biophys. Acta **23**, 260-264.

Glimcher MJ (1984) Recent studies on the mineral phase in bone and its possible linkage to the organic matrix by protein-bound phosphate bonds. Phil. Trans. R. Soc. London **B 304**, 479-508.

Green M, Isaac DH, Jenkins GM (1985) Bone microstructure by collagenase etching. Biomaterials **6**, 150-152.

Green M, Isaac DH, Jenkins GM (1988) Mineral structure and preferred orientation in the fin bones of the plaice, *Pleuronectes platessa*. Biomaterials **9**, 319-323.

Johansen E, Parks HF (1960) Electron microscopic observations on the three-dimensional morphology of apatite crystallites of human dentine and bone. J. Biophys. Biochem. Cytol. **7**, 743-745.

Münzberg KJ (1970) Untersuchungen zur Kristallographie der Knochenminerale (Study on the crystallography of the minerals in bone). Biomineralisation **1**, 67-100.

Robinson RA, Watson ML (1952) Collagen-crystal relationships in bone as seen in the electron microscope. I. Anat. Rec. **114**, 383-410.

Robinson RA (1955) Crystal-collagen relationships as observed in the electron microscope. III. Crystal and collagen morphology as a function of age. Ann. NY Acad. Sci. **60**, 596-628.

Schwarz W, Pahlke G (1953) Elektronenmikroskopische Untersuchungen an der Interzellularsubstanz des menschlichen Knochengewebes (Electron microscopic study on the intercellular substance of human bone tissue). Z. Zellforsch. **38**, 475-487.

Sela J, Boyde A (1977) Further observations on the relationship between the matrix and the calcifying fronts in osteosarcoma. Virchows Arch. A Path. Anat. and Histol. **376**, 175-180.

Stühler R (1938) Über den Feinbau des Knochens: Eine Röntgen-Feinstruktur-Untersuchung (On the fine structure of bone: an X-ray microstructural analysis). Fortschr. Gebiete Röntgenol. **57**, 231-264.

Thorogood PV, Gray JC (1975) Demineralization of bone matrix: observations from electron microscope and electron-probe analysis. Calcif. Tissue Res. **19**, 17-26.

Turner IG, Jenkins GM (1981) The spatial arrangement of bone mineral as revealed by ion bombardment. Biomaterials **2**, 234-239.

Walters MA, Leung YC, Blumenthal NC, LeGeros RZ, Konsker KA (1990) A Raman and infrared spectroscopic investigation of biological hydroxyapatite. J. Inorg. Biochem. **39**, 193-200.

Weiner S, Price PA (1986) Disaggregation of bone into crystals. Calcif. Tissue Int. **39**, 365-375.

Discussion with Reviewers

M.W. Lundy: The lamellar pattern of bone can be observed in polished specimens of bone, suggesting the amount of mineral and the structure of matrix are different in adjacent lamellae. Were differences in crystal structure or organization observed in bands that were 3-4 μm wide?

Authors: Our criteria for classifying surfaces were whether the surfaces were forming, resorbing, or resting. We did this for lamellar as well as for cancellous bone, with a view to try to establish discrete bone mineral particles, possessing grain boundaries. We did not study the samples with lamellar/interlamellar structure in mind.